8th ICFA Beam Dynamics Mini-Workshop on Two-Stream Instabilities in Particle Accelerators and Storage Rings

Wide Band BPM Measurements of Unstable PSR Beam.

A. Aleksandrov, V.Danilov, ORNL, Oak Ridge, TN

Abstract

This is a note on the processing of the signals from PSR strip line BPM that obtained in experiments on e-p instability. Algorithm of time resolving measurement of beam transverse position using wide band strip line pickup is presented. Two-dimensional Fourier transform of the signals in presence of the fast instability is analyzed.

I. Introduction

Precise measurement of beam centroid movement is very important for understanding the instability in the Proton Storage Ring (PSR). Fast strip line BPM (WM41) can provide this information if proper processing algorithm is used. In the previous work on this subject [1] vertical difference signal obtained by analog subtraction of signal from top and bottom strip lines of BPM was analyzed.

In this work we analyze signals from top and bottom strip lines digitized separately and make further processing in digital form to eliminate errors in frequency dependent analog hybrid. Suggested algorithm allows to calculate transverse beam position on each turn, than beam centroid movement on successive turns can be developed in series of plane travelling waves in beam frame of reference thus providing important information on instability development.

II. Calculation of beam displacement.

Voltage induced on strip line by moving charge can be expressed in terms of scalar product of charge velocity and static electric field of strip with unit potential. Beam moving with small angle along strip will excite it on the edges and net voltage across upstream port is [2]:

$$u(t) = I(t)F(x(t)) - I(t-\tau)F(x(t-\tau)), \qquad (1)$$

where $I(t)$ is beam current, $F(x)$ is function depending on strip line geometry , $x(t)$ is distance from beam centroid to strip line, τ is signal delay in strip line.

This expression is well applicable to the signal excited by proton beam in PSR but not to the signal excited by transversely moving electrons if they exist. Estimation of the electron contribution was done in [3].

Rewrite (1) in general form:

$$u(t) = U(t) - U(t-\tau)\,, \tag{2}$$

in the first order

$$u(t) = U(t) - U(t) + U'(t)\tau + ... \cong U'(t)\tau\,, \tag{3}$$

integrating both sides

$$u(t)dt = U(t)\tau\,, \tag{4}$$

we obtain the first order approximation expression for $U(t)$:

$$U_1(t) = \frac{1}{\tau} \quad u(t)dt \quad . \tag{5}$$

In order to calculate the accuracy of the first approximation we calculate Fourier transformation of (5):

$$\begin{aligned} \tilde{U}_1(\omega) &= \frac{1}{\tau}\frac{1}{\omega}\tilde{u}(\omega) = \frac{1}{\tau}\frac{1}{\omega}\left(\tilde{U}(\omega) - \tilde{U}(\omega)\cdot e^{-\omega\tau}\right) = \frac{\tilde{U}(\omega)}{\omega\tau}\cdot e^{-\frac{\omega\tau}{2}}\left(e^{\frac{\omega\tau}{2}} - e^{-\frac{\omega\tau}{2}}\right) = \\ &= \frac{\tilde{U}(\omega)}{\omega\tau}\cdot e^{-\frac{\omega\tau}{2}}\cdot 2\cdot\sin(\frac{\omega\tau}{2}) = \tilde{U}(\omega)\cdot H(\omega), \end{aligned} \tag{6}$$

Integration of BPM output signal is equivalent to applying a filter with transfer function $H(\omega)$ to beam signal $U(t)$, where

$$H(\omega) = \frac{2e^{-\frac{\omega\tau}{2}}}{\omega\tau}\sin(\frac{\omega\tau}{2}) \tag{7}$$

Note that linear dependence of the phase upon frequency leads to shift of the signal in time by $\frac{\tau}{2}$ not affecting its shape. The dependence of the absolute value of $H(\omega)$ upon frequency is shown in fig.1. Bandwidth at -3dBlevel is about 500MHz. Attenuation of high frequency harmonics doesn't affect beam position reconstruction directly if the ratio of two signals is used, but it affects accuracy by decreasing signal to noise ratio.

Using (5) we calculate voltage on top and bottom BPM strip lines, U_t and U_b respectively. Then beam centroid displacement can be derived from its ratio [3]:

$$y[mm] = 1.4737\cdot R - 0.00027\cdot R^3, \tag{8}$$

where $R = 20 \cdot \log(\frac{U_t}{U_b})$. Numerical coefficients here are derived from calibration data for this particular BPM.

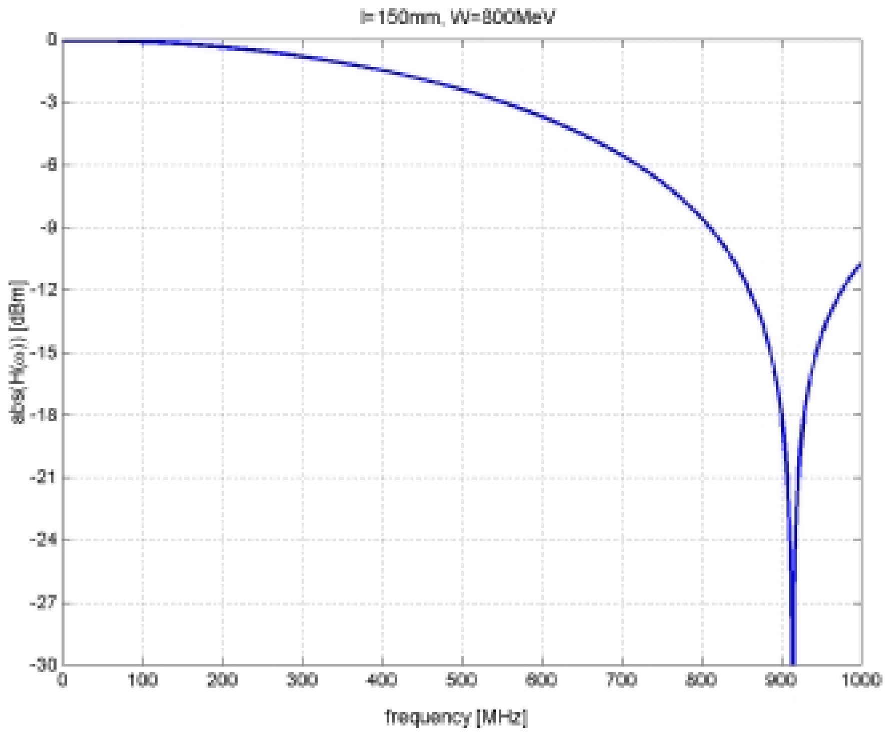

Figure. 1. Absolute value of the transfer function (7).

III. Measurement of the transverse beam position in the PSR storage ring.

The signals from top and bottom electrodes of WM41 strip line pickup were recorded by digital oscilloscope with 2Gs/s sample rate. Then original beam induced voltage was restored using (5). Example of recorded and restored waveform form the top electrode is shown in fig.2. Beam centroid displacement from BPM center was calculated using (8). Result for one turn is shown in fig.3. Blue line represents beam centroid displacement, red line is the sum of the signals from top and bottom electrodes, proportional to the beam current. One can see that oscillations develop on the trailing edge of the beam. In Figure 4 the amplitude of transverse oscillations of selected part of the beam versus number of turns is shown. The dashed straight line corresponds to the average growth of amplitude. The calculated increment of this instability is equal to 182 turns in this case.

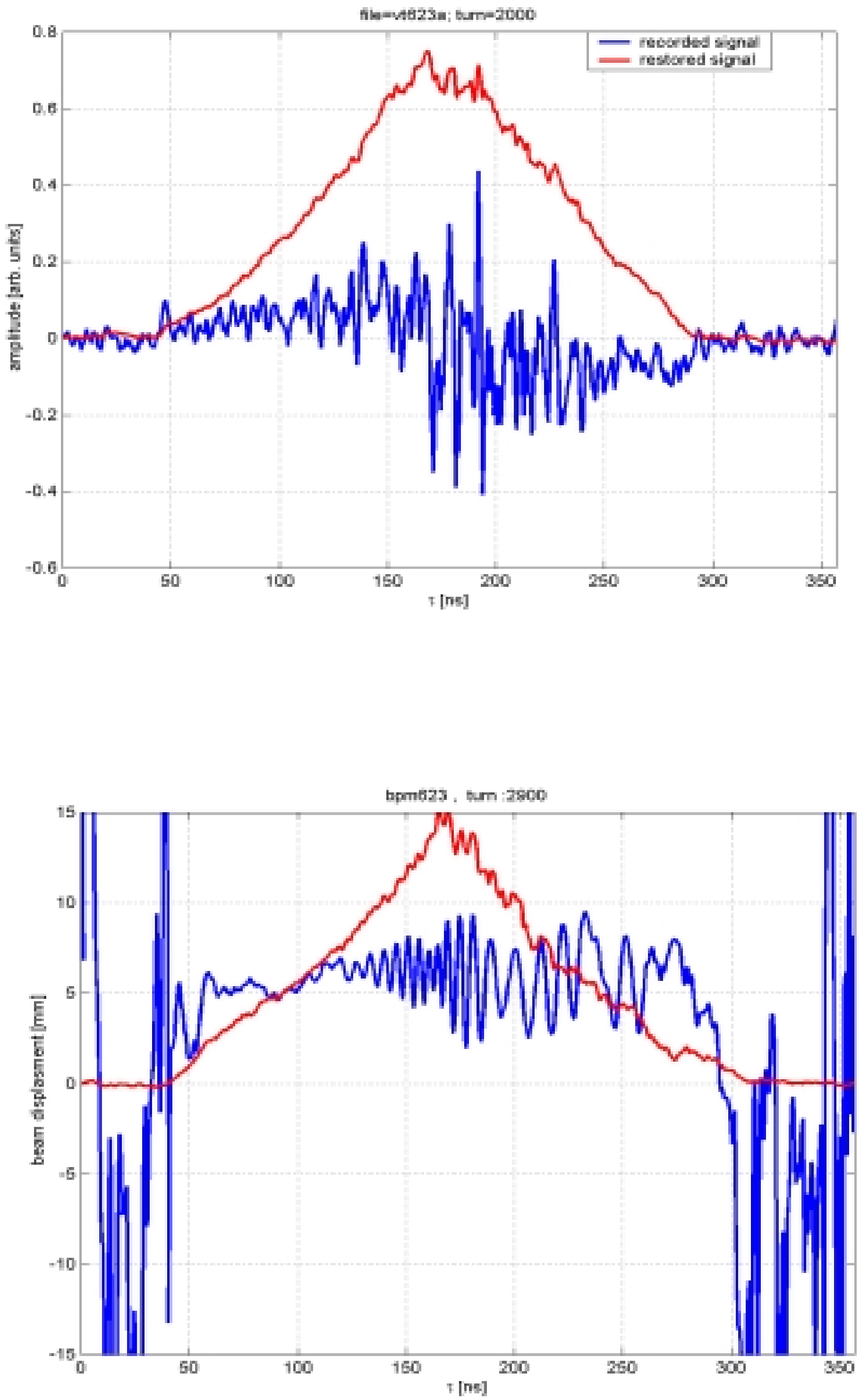

Figure 3. Beam centroid displacement (blue line) and beam current profile (red line) during one turn.

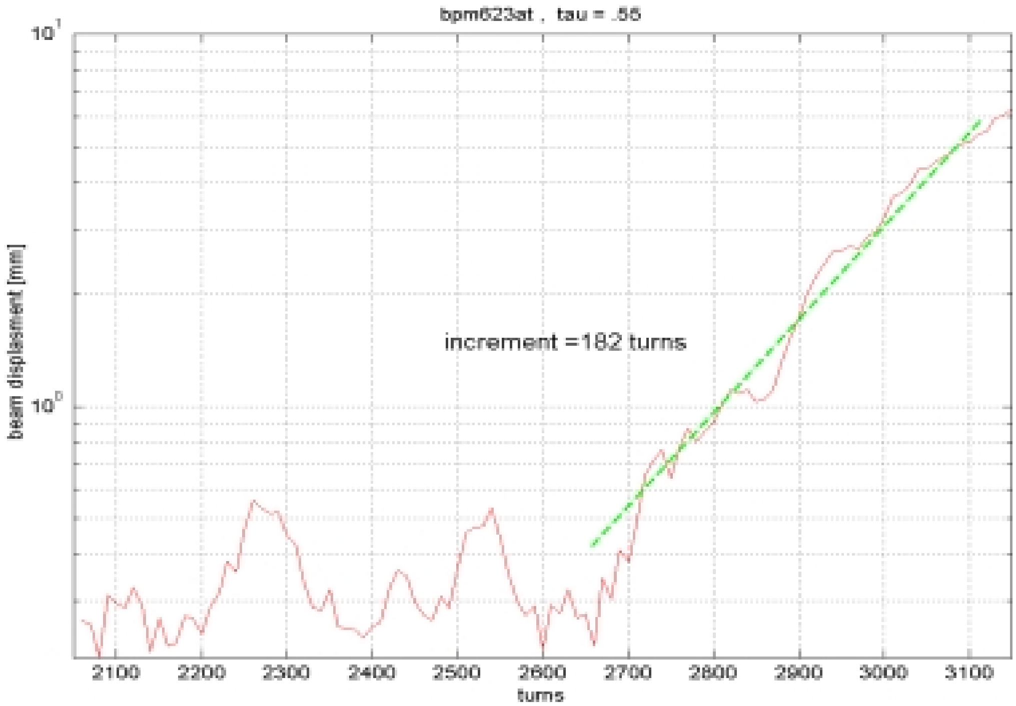

IV. Some observed properties of vertical transverse instability.

Vertical displacement of the beam centroid is different at different parts of the beam and it changes from turn to turn. In order to observe instability in a whole but not only at the selected turns or points the algorithm described below was developed.

1. Recorded stream is divided on pieces of N points corresponding to separate turns, 357.5 ns each.
2. M pieces (turns) are combined in N×M array of numbers A. Any single column represents signal at one turn. Any row represents signal from the selected beam point at successive turns.
3. Beam position is calculated applying (5), (8) to the array.

Figure 5 shows topographic view of the beam charge array calculated using described algorithm. Y-axis represents longitudinal position inside the beam, X-axis represents number of the turn. Figure 6 shows topographic map of the amplitude of the vertical oscillations. BPM readings have large error on the edges of the beam, where current is small (it can be seen in figs.4, 6). Therefore in further analysis a window (Hanning or square) was applied to every column to suppress noise at points where beam intensity is less than 10 % of its maximum.

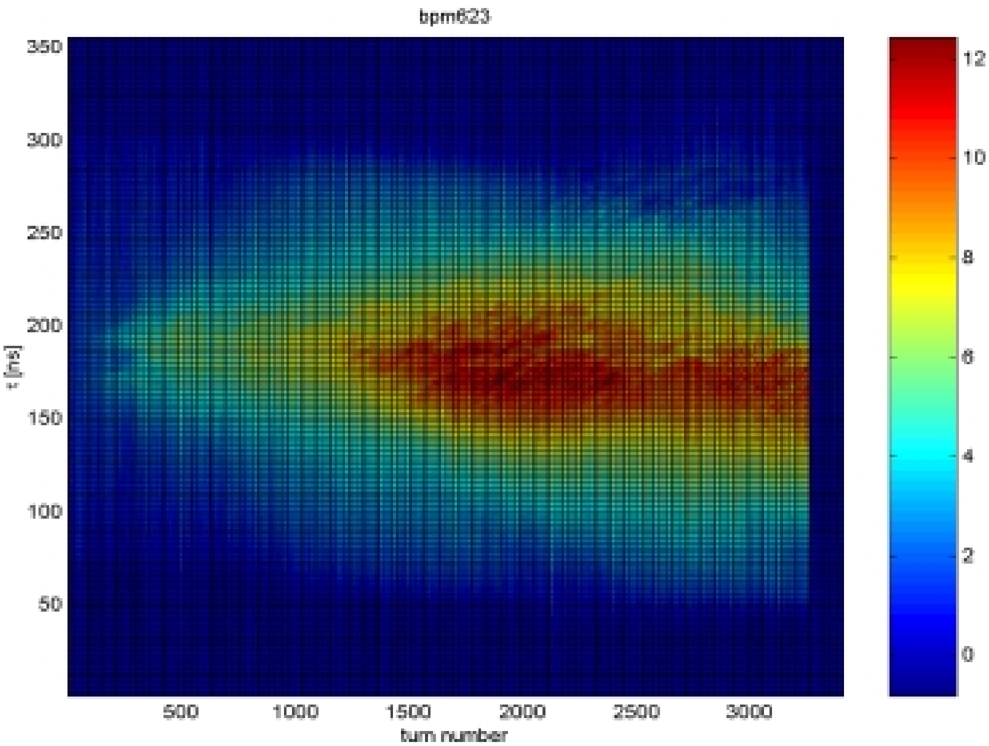

Figure 5. Topographic plot of beam current.

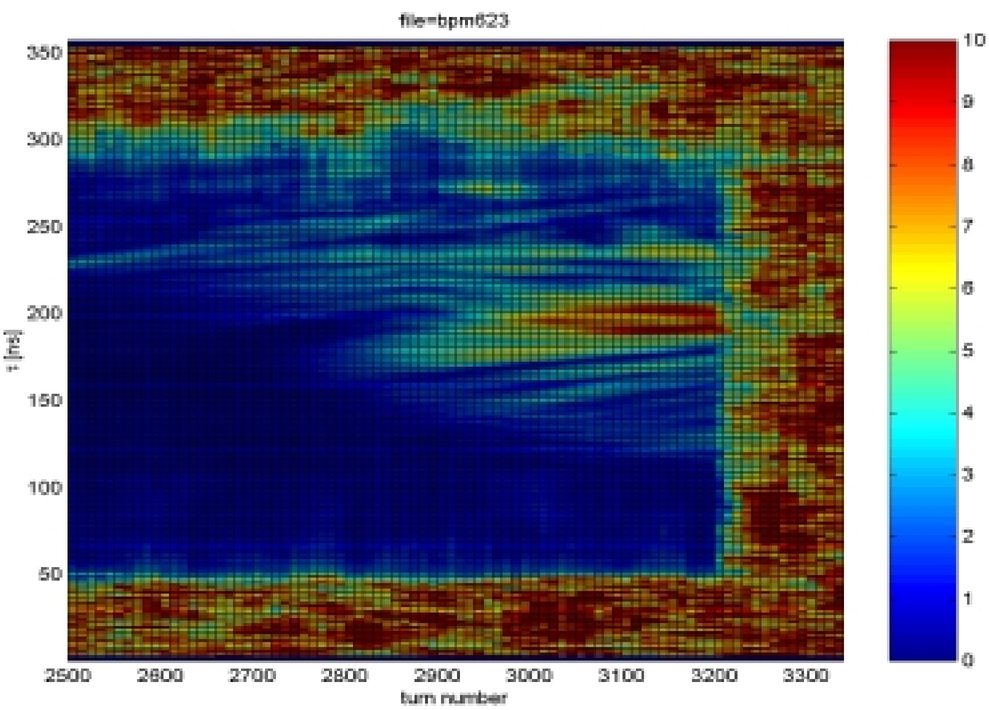

Figure 6. Topographic plot of beam centroid displacement.

One can develop observed picture of beam displacement in sum of plane travelling waves in the beam frame of reference by performing 2D Fourier transform on any N×m submatrix of the array A. Indeed, Fourier transform along a row contains $e^{-i\omega t}$ factor, Fourier transform along a column contains e^{-ikz} factor (where z is coordinate along the beam) and their product contains $e^{-i\omega t} \cdot e^{-ikz} = e^{-i(\omega t + kz)}$, that is a plane travelling wave (see also Appendix) . The result of 2D FFT on N×64 subarray with the instability present is shown on the contour plot in fig.7. The change of the color from blue to red corresponds to the increasing of the amplitude. The horizontal axis is the frequency, expressed in terms of the revolution frequency. The vertical axis is the spatial harmonic number that is the circumference of the PSR, divided by the wavelength of the harmonic. It's worth to note that only harmonics with opposite signs of ω and κ are present, which is well known feature of two-stream instability.

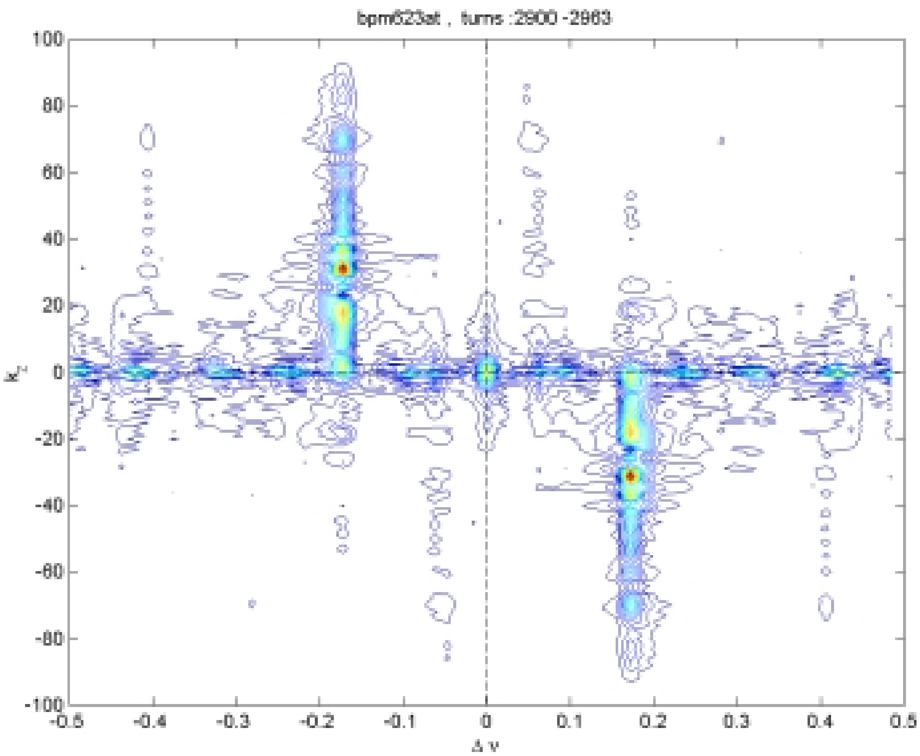

The instability increments are larger than 64 turns, so we can see its developing by analyzing a sequence of the adjacent arrays of 64 turns. In fig.8 development of instability is shown (only upper left quarter of full spectrum is plotted). Each subplot has the time difference of 100 turns with the previous one, with the a) subplot starting at 2400 turns from the beginning of the injection. The peaks with coordinates (0.18, k) correspond to the vertical betatron frequency. According to the "electron" explanation of this instability, the unstable harmonics should have spatial harmonic number close to the ratio of the electron bouncing frequency to the revolution frequency and they should have frequency near the betatron tune. That what we see on all plots of this figure.

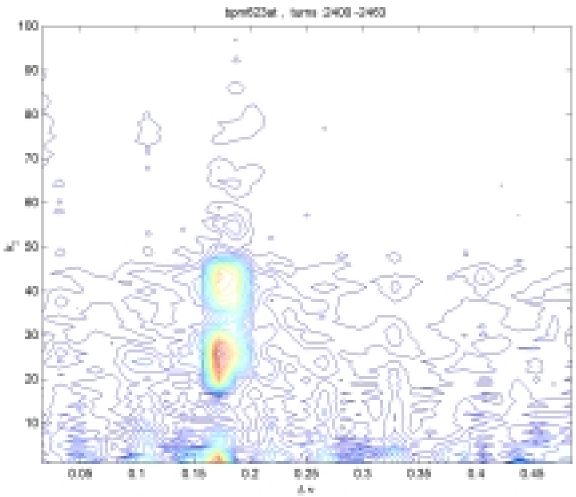
bpm623at , turns :2400 -2463
Δ ν

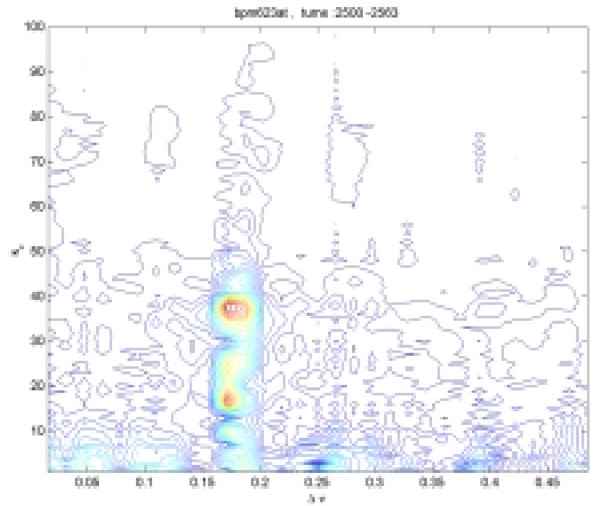
bpm623at , turns :2500 -2563
Δ ν

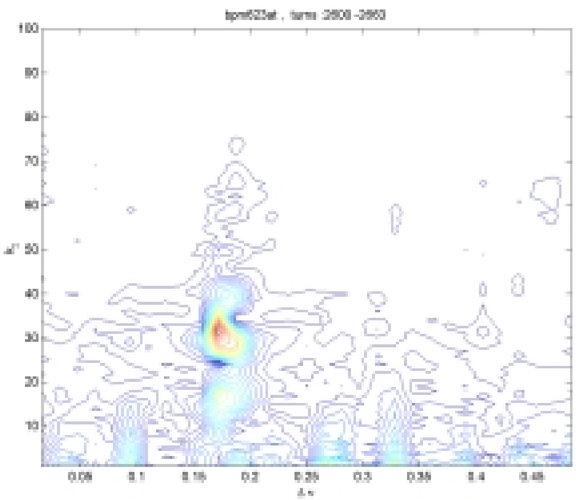
bpm623at , turns :2600 -2663
Δ ν

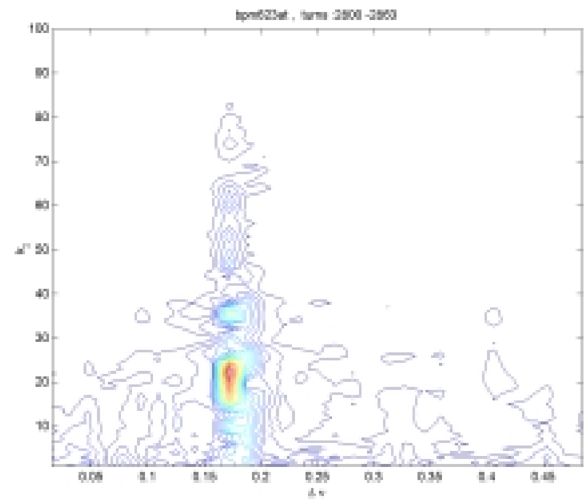
bpm623at , turns :2800 -2863
Δ ν

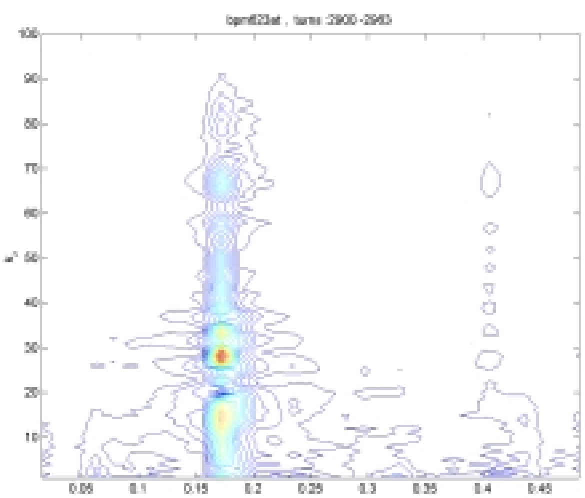
bpm623at , turns :2900 -2963
Δ ν

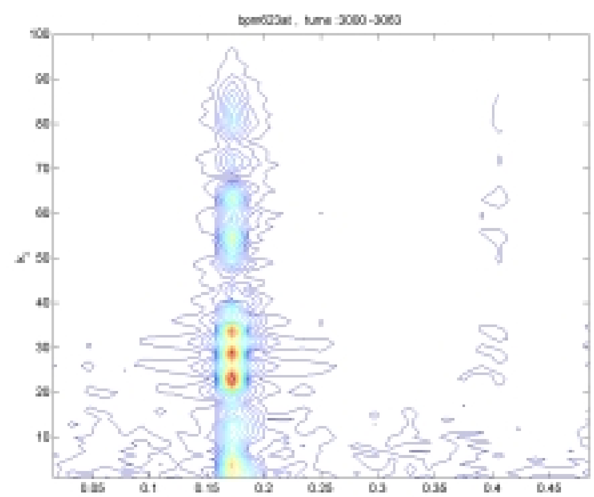
bpm623at , turns :3000 -3063
Δ ν

As only oscillations with betatron frequency are observed we can fix this number and to see how space harmonics number changes with time when instability develops. Result is shown on fig.9 as spectrogram of harmonic amplitude in coordinates (turn, k_z).

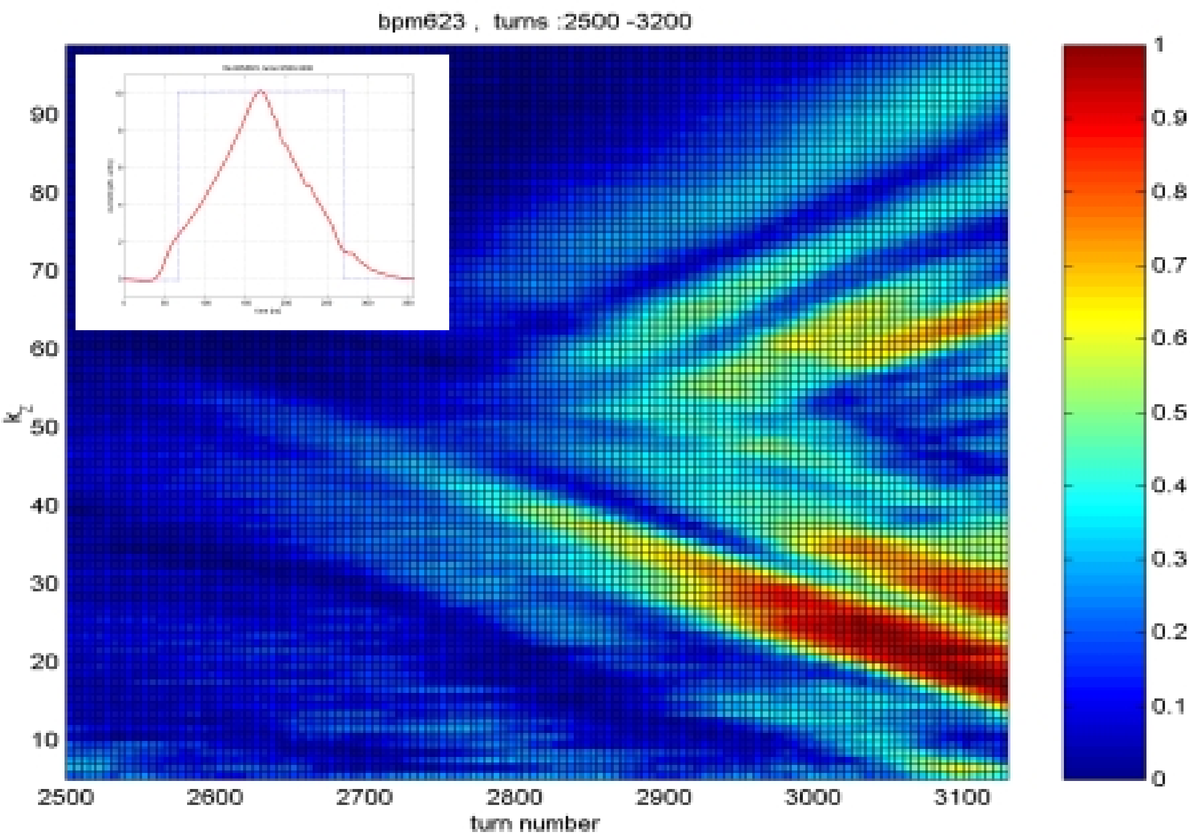

Figure 9. Spectrogram of spatial harmonics for the whole beam. Size and position of the window are shown in left upper corner.

Some very interesting features of the instability are observed:

1) ***Spectrum of space harmonics is discrete.***

2) ***There are two distinct regions of k_z: upper and lower with boundary near $k_z \approx 50$. k_z growth linearly with number of turns in the upper region and lowers in the lower region.***

In order to understand if those two regions correspond to different parts of the beam or to different unstable modes the same analysis was done using FFT with narrow window. In the first case window was centered on the leading edge of the beam, in the second case it was centered on the trailing edge. The results are shown in figs. 10,11 correspondingly. It is seen clearly that upper region of k_z corresponds to leading edge and lower region corresponds to trailing edge of the beam. In order to investigate the dependence of the frequency upon charge density, the spatial frequency was measured at different points of the beam during single turn using FFT with sliding window.

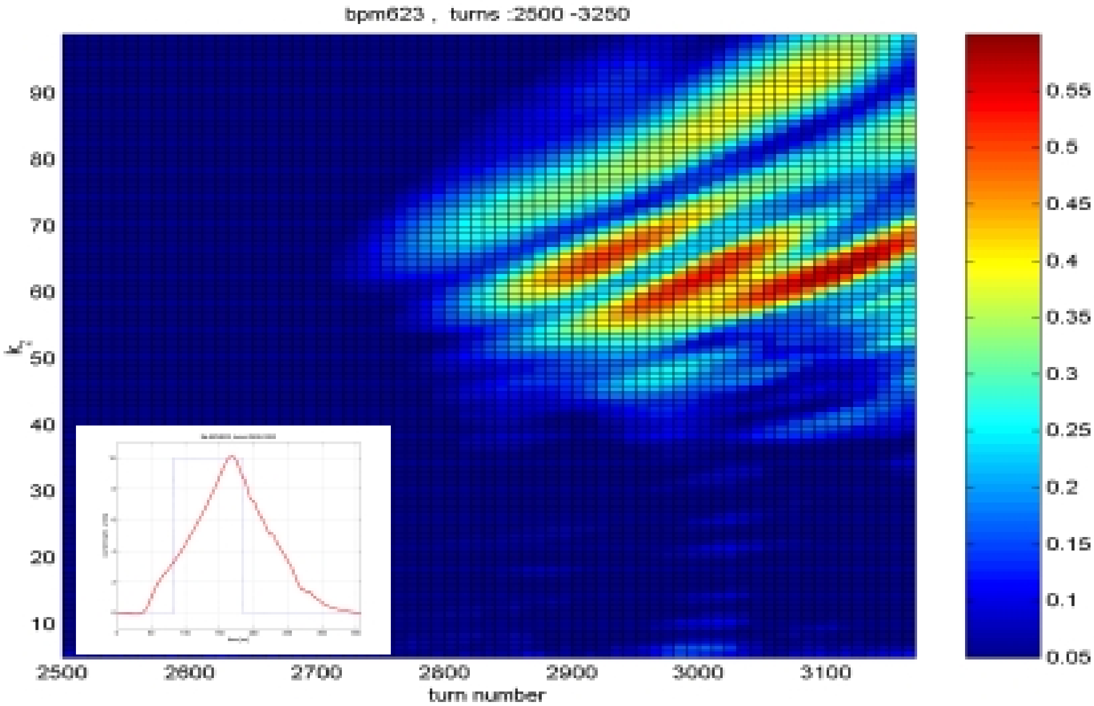

Figure 10. Spectrogram of spatial harmonics for the leading edge of the beam. Size and position of the window are shown in left lower corner.

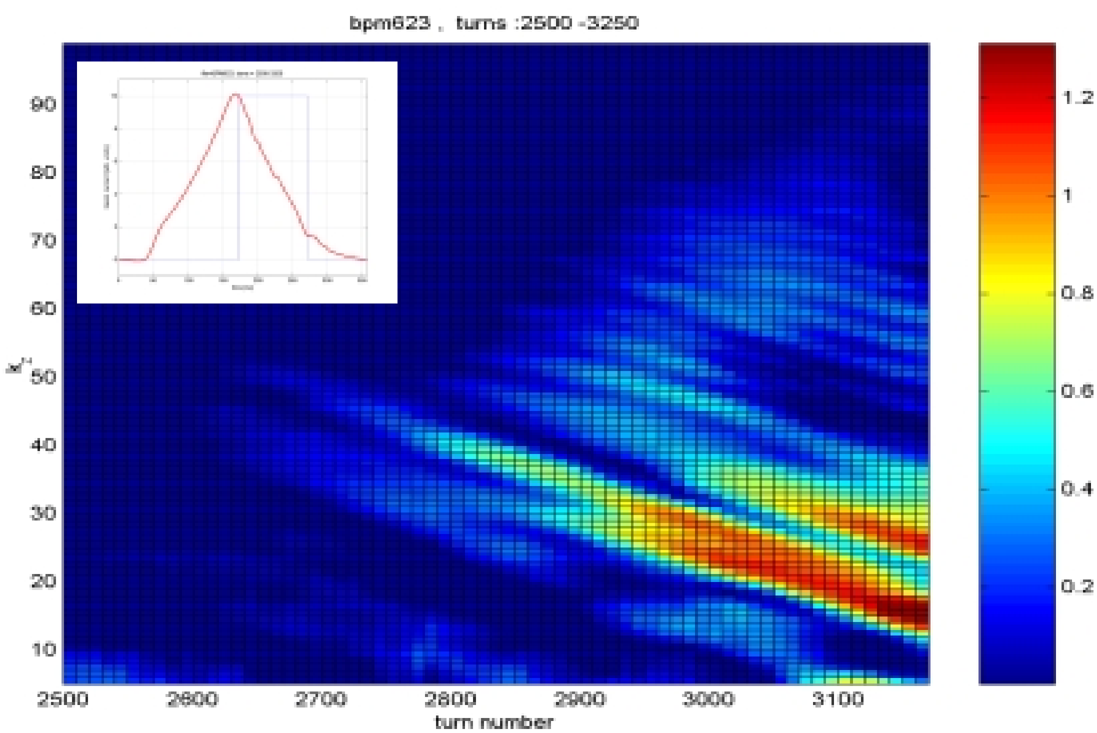

Figure 11. Spectrogram of spatial harmonics for the trailing edge of the beam. Size and position of the window are shown in left upper corner.

The result averaged for five successive turns is shown in figs. 12,13. Fig.13 shows spatial harmonic number normalized on square root of the beam current (red curve) and on beam current (blue curve) is shown. Qualitatively k_z is proportional to I_b on the leading edge of the beam and to square root of I_b on the trailing edge. Note that we use measured current of the proton beam for normalization but charge density can be different due to neutralization from electron cloud or due to beam transverse size variation along the beam.

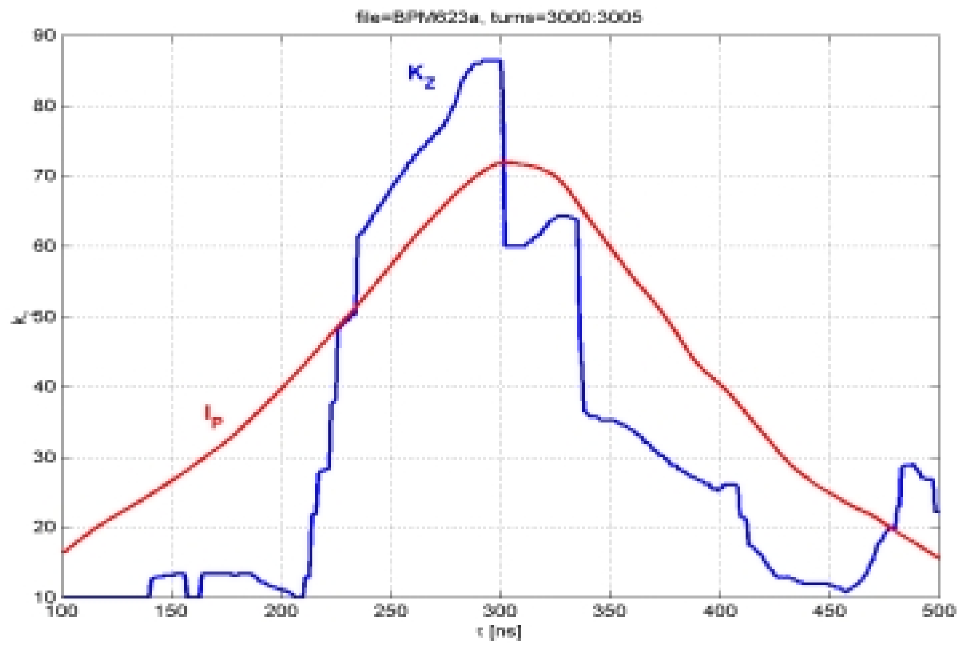

Figure 12. Resonant harmonic number versus position inside the beam.

3) Spatial harmonic number k_z changes with number of turns linearly. It means that unstable harmonic can not be described by plane wave with constant frequency and wave number as in the case of coasting beam.

Assuming "electron cloud" nature of the instability we can explain observed decreasing of the resonant frequency by decreasing of electron "bouncing frequency" due to space charge density decreasing. Space charge density can decrease due to neutralization from electron cloud or due to increasing of transverse beam size. Time resolving measurement of electron charge collected by the electron detectors [4] says in favor of neutralization hypotheses. In this case we can estimate the upper limit of instability threshold in the following way.

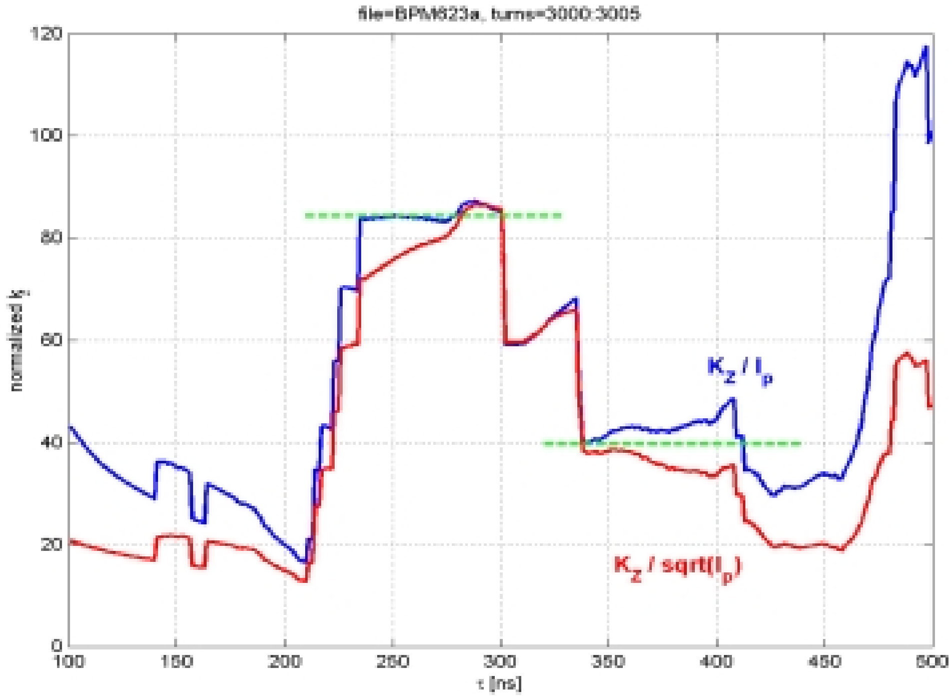

Figure 13. Resonant harmonic number normalized on beam current versus position inside the beam.

V. Conclusion.

We have presented a method of PSR fast BPM signal processing which allows restoring beam centroid transverse movement in time domain. It provides a powerful tool for PSR instability study. Some new results of beam movement analysis are presented.

VI. Acknowledgements.

We wish to thank Robert Macek who initiated this work and provided experimental data from PSR storage ring.

VII. References:

[1] Tai-Sen F. Wang, Technical Note: PSR-93-024, 1993
[2] K.-Y. Ng, Fields, Impedances and Structures
[3] J.D. Gilpatrick, Technical Note: LA-CP-97-21, 1997
[4] A. Browman, Electron measurements at PSR, presented at this Workshop.

Appendix.

Due to beam movement along orbit data acquired by one BPM at fixed point do not represent centroid position of all points of the beam in one moment of time. Let $x_0(t,s)$ be beam centroid transverse position in beam frame of reference, where *s* is coordinate along orbit varying from 0 to orbit circumference $2\pi R$. Then BPM will measure in laboratory frame of reference transverse position $x=x_0(t + s/v, s)$, where v is beam velocity. Fourier transform of x is:

$$X(\omega, s) = F_t(x) = F_t(x_0(t + s/\mathrm{v}, s)) = F_t(x_0) \cdot e^{i\omega\frac{s}{\mathrm{v}}} = X_0(\omega, s) \cdot e^{i\omega\frac{s}{\mathrm{v}}},$$

then Fourier transform along s is

$$X(\omega, k) = X_0(\omega, k + \frac{\omega}{v})$$

In approximation of smooth focusing $\omega=\omega_\beta$, therefore

$$X(k) = X_0(\omega_\beta, k + \frac{\omega_\beta}{v}).$$

It means that spectrum of spatial harmonics obtained from BPM signal differs from spectrum of bunch “snap-shot” by the constant shift of $\frac{\omega_\beta}{v}$.